

Seismic response of 3D steel buildings with hybrid connections: PRC and FRC

Alfredo Reyes-Salazar^{*}, Jesús Alberto Cervantes-Lugo^a,
Arturo López Barraza^b, Edén Bojórquez^c and Juan Bojórquez^d

Facultad de Ingeniería, Universidad Autónoma de Sinaloa, Ciudad Universitaria, Culiacán Sinaloa, México

(Received July 07, 2016, Revised September 20, 2016, Accepted September 22, 2016)

Abstract. The nonlinear seismic responses of steel buildings with perimeter moment resisting frames (PMRF) and interior gravity frames (IGF) are estimated, modeling the interior connections first as perfectly pinned (PPC), and then as partially restrained (PRC). Two 3D steel building models, twenty strong motions and three levels of the PRC rigidity, which are represented by the Richard Model and the Beam Line Theory, are considered. The RUAUMOKO Computer Program is used for the required time history nonlinear dynamic analysis. The responses can be significantly reduced when interior connections are considered as PRC, confirming what observed in experimental investigations. The reduction significantly varies with the strong motion, story, model, structural deformation, response parameter, and location of the structural element. The reduction is larger for global than for local response parameters; average reductions larger than 30% are observed for shears and displacements while they are about 20% for bending moments. The reduction is much larger for medium- than for low-rise buildings indicating a considerable influence of the structural complexity. It can be concluded that, the effect of the dissipated energy at PRC should not be neglected. Even for connections with relative small stiffness, which are usually idealized as PPC, the reduction can be significant. Thus, PRC can be used at IGF of steel buildings with PMRF to get more economical construction, to reduce the seismic response and to make steel building more seismic load tolerant. Much more research is needed to consider other aspects of the problem to reach more general conclusions.

Keywords: steel buildings; partially restrained connections; energy dissipation; nonlinear seismic response; global and local response parameters

1. Introduction

The devastating effects caused by large-scale seismic events on structures in several parts of the world during the last decades, have originated an intensification of earthquake engineering research in recent years. Steel buildings have not been the exception; extensive damage was

^{*}Corresponding author, Professor, E-mail: reyes@uas.edu.mx

^a Ph.D. Student, E-mail: beto_donai@hotmail.comx

^b Ph.D., E-mail: alopezb@uas.edu.mx

^c Professor, E-mail: eden@uas.edu.mx

^d Ph.D., E-mail: jbm_squall_cloud@hotmail.com

observed in beam-column welded connections in moment-resisting frames (MRF) during the Northridge Earthquake of 1994 and the Kobe Earthquake of 1995. One of the typically damaged steel beam-column connections was the bolted-web, welded-flange connection. Brittle fractures initiated within this type of connections at very low levels of plastic demand, and in many cases, while the structures remained essentially elastic. Fractures initiated at the complete joint penetration weld between the beam bottom flange and column flange. This forced researchers and structural engineers to reexamine seismic design practices existed before these events and to look for different structural configurations, structural systems, materials and alternative connections, to improve structural behavior during intense seismic excitations.

The use of MRF in steel buildings has been popular because they provide maximum flexibility for space utilization and because of their high ductility capacity. The characteristics of the basic structural system, however, have significantly changed over the years in some developed countries like USA. From the mid 60s to the mid 70s, most connections were assumed to be fully restrained (FRC). In the recent past, the use of FRC were considerably reduced because they were expensive and to eliminate weak-axis connections (FEMA 2000); FRC are used only on two frame lines in each direction, usually at the perimeter (PMRF). As a result of this structural arrangement, the redundancy of the building is significantly reduced. An important issue that deserves our attention is that PMRF are usually designed as plane frames to resist the total lateral seismic loading, ignoring the presence of interior gravity frames (IGF), which are designed to resist only the gravity loads. Due to the action of the rigid floor diaphragm, the IGF, however, will undergo the same lateral deformation as the PMRF, developing bending moments and shear forces in columns. Therefore, the contribution of IGF to the lateral resistance of the building could be significant, particularly for buildings with relatively few FRC. In addition, the beam-to-column connections of the IGF are assumed to be perfectly pinned (PPC) when in reality they are partially restrained (or semi-rigid) connections (PRC). Modeling a connection to be either FRC or PPC type is simply an assumption made to simplify calculations and it is a major weakness in current analytical procedures. One of the major implication of this is that the dissipated energy at the interior PRC is not considered but it could have an important effect on the structural response. Consideration of the rigidity of the connections of the IGF as PRC, and other aspects as energy dissipation on them, as will be further discussed below, constitutes the main objective of this paper.

Because of the observed damage, several researchers have suggested replacing welded connections for bolted PRC, since they could dissipate more hysteretic energy, attract less inertial forces and undergo stable cyclic response. It is also argued that, if designed properly, bolted PRC may have high ductility and cyclic-energy-dissipation capacity eliminating the brittle failure observed in welded connections; at the same time they can provide the same stiffness as steel buildings with fewer frames with FRC in such a way that their performance may be equal or superior to that of FRC buildings. Additionally, it is stated that today much more is known about the stiffness and strength properties of PRC than was known at the time when fully FRC was the standard connection in highly seismic regions. However, the use of steel buildings with PRC in high seismicity areas has not been broadly generalized; there is the belief that there is a reduction of their overall structural stiffness and consequently the displacements will significantly increase when compared to those of typical building with FRC. As it is elaborated further below, the central objective of this paper is related to the non-linear seismic response estimation of steel buildings consisting of a hybrid system with interior PRC and exterior FRC, where the stiffness and the dissipated energy of the PRC are explicitly considered.

2. Literature review

The seismic behavior of steel buildings with MRF has been a research topic of interest to the profession during the last few decades. Lee and Foutch (2006) studied the seismic behavior of 3-, 9-, and 20-story MRF designed for different reduction factors. Krishnan *et al.* (2006) determined the damage produced by hypothetical earthquakes on two 18-storey MRF, one existing and one improved according to the Uniform Building Code (1997), located in southern California, USA. Liao *et al.* (2007) developed a three-dimensional finite-element model to examine the effects of bi-axial motion and torsion on the nonlinear response of MRF. Effects of gravity frames, panel zones, and inelastic column deformation were considered. More recently, Chang *et al.* (2009), by using 6- and 20-level steel office buildings, studied the role of accidental torsion in seismic reliability assessment. Bojorquez *et al.* (2010) found that moment resisting steel plane frames are very efficient in dissipating earthquake-induced energy and that the dissipated energy has an important effect on the structural response. Garcia *et al.* (2010) proposed a Displacement-Based Design methodology for steel frame-RC wall structures. Their structural performance was investigated through nonlinear time-history analyses by using seven spectrum-compatible accelerograms. Black (2012) used regression analysis of data collected from nonlinear static and modal analysis of 22 steel MRF to propose empirical equations to estimate key inelastic parameters, as frame's yield displacement and strength. Reyes-Salazar *et al.* (2015), studied the ductility reduction factor for steel buildings with MRF which were modeled as complex MDOF systems, considering an intermediate level of inelastic structural deformation. They showed that the ductility reduction factors associated to global response parameters may be quite different than those of local response parameters.

The seismic behavior of steel buildings with PRC and the effect of the dissipated energy on their response have also been studied by many researchers. It has been established, both theoretically and experimentally, that these connection exhibit semi-rigid nonlinear behavior even if the applied loads are very small (Reyes-Salazar and Haldar 2000). The contribution of these connections to the structural strength and stiffness can be much important if the composite action of the concrete slab is considered (Reyes-Salazar and Haldar 1999, Liu and Astaneh-Asl 2000). Bjorhovde *et al.* (1990) developed a scheme where connections are classified in terms of strength, stiffness, and ductility, according to tests and theoretical data. The classification system is arranged in such a way that new connection types can be easily fitted into the current data base. Elnashai and Elghazouli (1994) studied the performance of a two-storey with rigid and semi-rigid connections. The numerical and experimental results showed that semi-rigid frames exhibits ductile and stable hysteretic behavior and may be effectively used in earthquake resistance design. Elnashai *et al.* (1998) presented the results of the experimental results dealing with the seismic behavior of semi-rigid steel frames with top, seat, and web angles. It was shown that the type of the bolted connection used in this study exhibits sufficient ductility and stable hysteretic behavior and that connection yielding is a viable alternative to the weak-beam strong-column design.

In another studies (Nader and Astaneh-Asl 1991, Leon and Shin 1995, Reyes-Salazar and Haldar 2000) it was shown that the maximum values of base shear and interstory displacements of plane steel frames under earthquake ground motions were reduced when PRC were used. The reason for this is that the frames with PRC connections dissipate more energy and attract less inertial forces than frames with FRC (Reyes-Salazar and Haldar 2000). Kishi *et al.* (1996) investigated the reduction in costs of tall buildings with mixed FRC and PRC connections. Kishi *et al.* (2003) proposed an useful design aid for determining the values the connection parameters with

the help of a set of monographs which allows the engineer to rapidly determine the Moment-Rotation curve for a given connection. Experimental tests with angle connections, subjected to cyclic and monotonic loads conducted by Shen and Astanteh-Asl (1999, 2000) showed a stable cyclic response and good capability of hysteretic energy dissipation. The state of the art report “seismic performance of steel moment frames subjected to earthquake ground motion shaking” (FEMA 2000) under the leadership of Professor Krawinkler represents a major step in the advance of the understanding of the seismic behavior of steel buildings with FRC and PRC. However, as stated in the report itself, the study on the effect of interior gravity columns and their shear connections on the seismic response, was limited since this effect was approximately considered by using a 2-D model and a single column (“flag pole”). More recently Nguyen and Kim (2013) presented a simple effective numerical procedure based on the beam-column method for nonlinear elastic dynamic analysis of three-dimensional semi-rigid steel frames. The nonlinear elastic dynamic analysis results were compared with those of previous studies and commercial SAP2000 software to verify the accuracy and efficiency of the proposed analysis. Valipour and Bradford (2013) presented a formulation to consider the flexural and axial stiffness of the connections of plane steel frames, which is verified by using some numerical examples. Rafiee *et al.* (2013) proposes an optimization algorithm for optimal design of non-linear steel frames with semi-rigid beam-to-column connections, which obtains the minimum total cost; three design examples of plane frames with various types of connections are presented and the results show the efficiency of using semi-rigid connection models in comparing to rigid connections. Nguyen and Kim (2014) proposed a numerical procedure based on the beam-column method and based-displacement finite element method for nonlinear inelastic time-history analysis of three-dimensional semi-rigid steel frames, considering the nonlinear geometry and the inelasticity of material. The results are compared with those of previous studies. A nonlinear inelastic time-history analysis procedure for space semi-rigid steel frames subjected to dynamic loadings is proposed by Nguyen and Kim (2015); three main sources of inelastic hysteretic, nonlinear connecting, and structural viscous damping are considered. The nonlinear time-history responses compare well with those given by commercial finite element packages and other available results. Sagiroglu and Aydin (2015) proposed a computer-based analysis and design for three-dimensional steel frames with semi-rigid connections consisting of top and bottom angles with a double web angle connection. Various design examples are presented to demonstrate the efficiency of the method. Gholipour *et al.* (2015) investigated the seismic performances of dual steel moment-resisting frames with rigid and semi-rigid connections. They showed that it could be found a state of semi-rigidity and connections configuration which behaves better than rigid frame, with consideration of the base shear and story drifts criterion. Lopez-Barraza *et al.* (2016) studied the seismic responses in terms of hysteretic energy of five welded plane steel frames with post-tensioned PRC.

It is clear that, in order to properly capture the effect of the connections of the interior gravity frames on the structural response, they must be modeled as PRC within a three-dimensional (3D) complex MDOF structural representation of the buildings. PRC are mainly considered in two ways; the first one considers the connection as a single piece, and describes its behavior through the moment-relative rotation ($M-\theta_r$) curve (Reyes-Salazar and Haldar 2000, Yang and Jeon 2009, Richard and Abbot 1975, Richard 1993). The curve equation parameters are usually obtained from experimental results for a variety of PRC. In the second option, the parts of the connection are modeled with finite elements using fiber elements, assigning to each fiber a force-displacement relationship (Shen and Astanteh-Asl 2000, Ricles *et al.* 2001). The first option has the advantage that when implemented it in a frame analysis program, the number of elements required is

relatively smaller and therefore is adopted in this study. In this paper, all interior gravity columns and all their connections are explicitly considered in a 3D complex MDOF structural model. The loading and unloading process at PRC and consequently their dissipated energy is explicitly considered too.

In spite of the important contributions of the earlier studies regarding the seismic behavior of steel buildings with FRC and PRC, more of them are limited to SDOF or to simplified plane models or to structural sub-assemblies. Moreover, results in terms of local response parameters, different levels of the interior connection rigidity as well as the modeling of the buildings as 3D complex MDOF systems, have not been considered. It is important to emphasize that modeling structures as SDOF or plane systems may not represent their actual behavior since the participation of some elements are not considered and the contribution of some vibration modes are ignored. The dynamic properties in terms of stiffness, mass distribution, natural frequencies and energy dissipation characteristics of buildings modeled as simplified systems are expected to be quite different than those resulting from a 3D modeling of the buildings. Reyes-Salazar and Haldar (1999, 2000, 2001a, b) found that moment resisting steel frames are very efficient in dissipating earthquake-induced energy and that the dissipated energy has an important effect on the structural response. Reyes-Salazar (2002) showed that the seismic response depends on the amount of dissipated energy, which in turn depends on the plastic mechanism formed in the frames as well as on the loading, unloading and reloading process at plastic hinges. It is not possible to consider these issues by using simplified models, particularly SDOF systems. Due to advancement in computer technology, the computational capabilities have significantly increased in the recent years. It is now possible to estimate the seismic response behavior by modeling structures as complex 3D MDOF systems with thousand of degrees of freedoms and applying the seismic loadings in time domain as realistically as possible. Responses obtained in this way may represent the best estimate of the seismic responses. The accuracy of estimating the seismic response of steel building with PRC and FRC by considering simplified SDOF or simplified plane systems can be judged by comparing the results with those obtained from the complex 3D MDOF formulation.

3. Objectives

The earlier discussion clearly indentify several issues, regarding the seismic behavior of 3D steel buildings with interior PRC and exterior FRC, that need to be studied. The particular objectives addressed in this study are: (a) to estimate the seismic responses, in terms of global response parameters, of the buildings considering the interior connections as perfectly pinned and compare them with those responses of the same buildings but considering the connections as semi-rigid, different levels of the connection stiffness and strong motion intensity levels are considered; (b) to compare the responses of the steel buildings, as above, but now in terms of local response parameters.

4. Methodology

4.1 Parameters of the study

Two 3D steel building models under the action of twenty strong motion earthquakes are considered in the study. The earthquakes are scaled down and up to produce six levels of structural

deformation. The steel building models are assumed to have, first interior PPC and then interior PRC. Three levels of rigidity, which is represented by the T ratio, are considered for the PRC oriented in the $E-W$ direction (strong direction) but only one level for the other direction. The responses are expressed in terms of global (lateral interstory displacements and interstory shears) and local response parameters (axial loads and bending at particular structural members).

4.2 Structural models

For numerical evaluation of the issues discussed earlier, the nonlinear seismic responses of two steel buildings with PMRF, which were used in the SAC steel project (FEMA 2000), are considered in this study. Particularly the 3- and 10-level buildings located in the Los Angeles area

Table 1 Lateral vibration periods

T Ratio	Lateral vibration periods (sec)					
	3-level model			10-level model		
	Mode I	Mode II	Mode III	Mode I	Mode II	Mode III
0	1.03	0.30	0.15	2.41	0.89	0.50
0.2	0.96	0.29	0.14	2.31	0.84	0.47
0.4	0.94	0.29	0.14	2.26	0.82	0.46
0.6	0.92	0.28	0.13	2.22	0.81	0.45

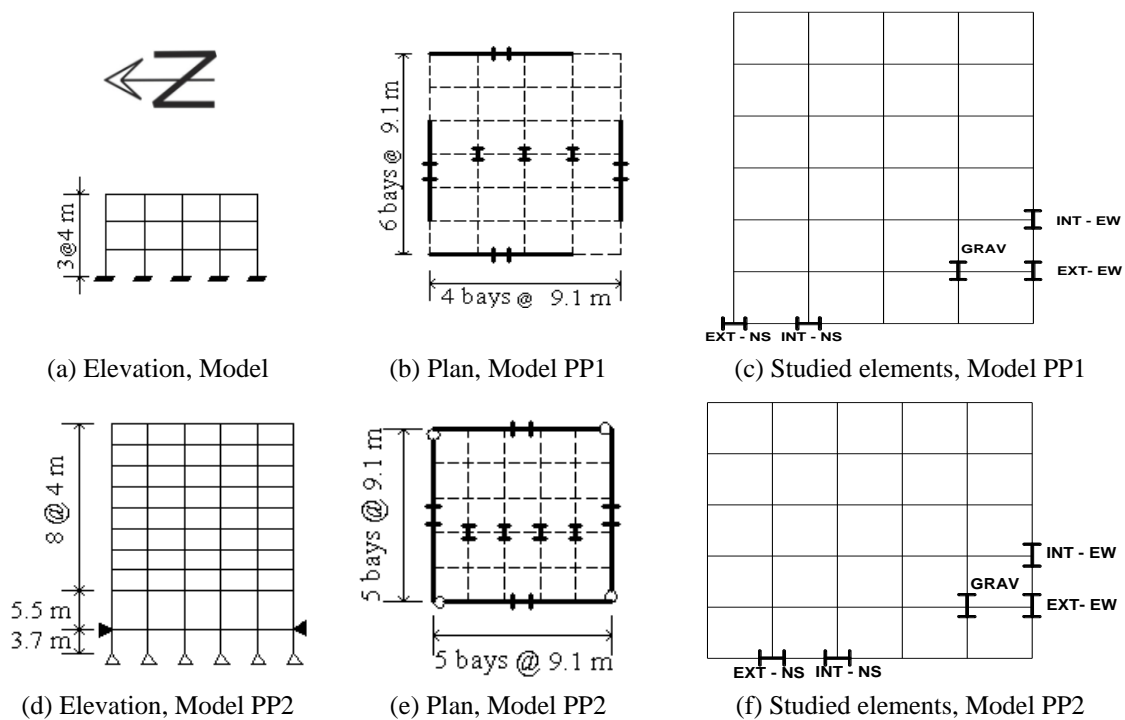


Fig. 1 Elevation, plan and element location for the PP Models

are studied. These buildings are supposed to satisfy all code requirements existed at the time of the project development for Los Angeles (UBC 1995), Seattle (UBC 1995) and Boston (BOCA 1993). The RUAUMOKO Computer Program (Carr 2011) is used for the required time history nonlinear dynamic analysis. The 3- and 10-level buildings with interior pinned connections will be denoted as Models PP1 and PP2, respectively, and in general, they will be referred as the PP Models. The first three vibration periods associated to lateral vibration of these models are given in Table 1 and their elevations and plans are given in Figs. 1(a), (b), (d), and (e). The T ratio is quantitatively defined below.

The particular elements to study the response in terms of local responses parameters are given in Figs. 1(c) and (f) for Models PP1 and PP2, respectively. In these figures, the PMRF are represented by continuous lines while the IGF are represented by dashed lines. Sizes of beams and columns, as reported (FEMA 2000), are given in Table 2 for the two models. In all these frames, the columns are made of steel Grade-50 and the girders are of A36 steel. For both models, the columns in the IGF are considered to be pinned at the base. The designs of the PMRF in the two orthogonal directions were practically the same. The damping is considered to be 3% of the critical. Additional information about the models can be obtained from the FEMA report. The buildings are modeled as complex MDOF systems. Each column is represented by one element and each girder of the PMRF is represented by two elements, having a node at the mid-span. The connections are represented by a nonlinear element (spring) whose properties are calculated by using the Richard Model (Richard 1993). The Ruaumoko Computer Program doesn't include the Richard Model, but

Table 2 Beam and columns sections for the SAC models

Model	Moment resisting frames				Gravity frames		
	Story	Columns		Girder	Columns		Beams
		Exterior	Interior		Below penthouse	Others	
1	1\2	W14×257	W14×311	W33×118	W14×82	W14×68	W18×35
	2\3	W14×257	W14×312	W30×116	W14×82	W14×68	W18×35
	3\Roof	W14×257	W14×313	W24×68	W14×82	W14×68	W16×26
2	-1/1	W14×370	W14×500	W36×160	W14×211	W14×193	W18×44
	1/2	W14×370	W14×500	W36×160	W14×211	W14×193	W18×35
	2/3	W14×370	W14×500, W14×455	W36×160	W14×211, W14×159	W14×193, W14×145	W18×35
	3/4	W14×370	W14×455	W36×135	W14×159	W14×145	W18×35
	4/5	W14×370, W14×283	W14×455, W14×370	W36×135	W14×159, W14×120	W14×145, W14×109	W18×35
	5/6	W14×283	W14×370	W36×135	W14×120	W14×109	W18×35
	6/7	W14×283, W14×257	W14×370, W14×283	W36×135	W14×120, W14×90	W14×109, W14×82	W18×35
	7/8	W14×257	W14×283	W30×99	W14×90	W14×82	W18×35
	8/9	W14×257, W14×233	W14×283, W14×257	W27×84	W14×90, W14×61	W14×82, W14×48	W18×35
9/Roof	W14×233	W14×257	W24×68	W14×61	W14×48	W16×26	

Table 3 PRC components

T ratio	Section	Web angle		Top and seat angles		Web bolts		Top and seat bolts	
		Size (in)	Length (in)	Size (in)	Length (in)	Number	Gage (in)	Number	Gage (in)
0.2	W16×26	4×4×3/8	11	NA	NA	5	2.5	NA	NA
	W18×35	4×4×3/8	11	NA	NA	5	2.5	NA	NA
0.4	W16×26	4×4×1/4	9	5×5×5/16	5.5	3	2	2	2.5
	W18×35	4×4×1/4	9	5×5×5/16	6	3	2	2	2.5
0.6	W16×26	4×4×3/8	9	5×5×5/16	5.5	4	2	2	2.5
	W18×35	4×4×3/8	9	5×5×3/8	6	4	2	2	2.5

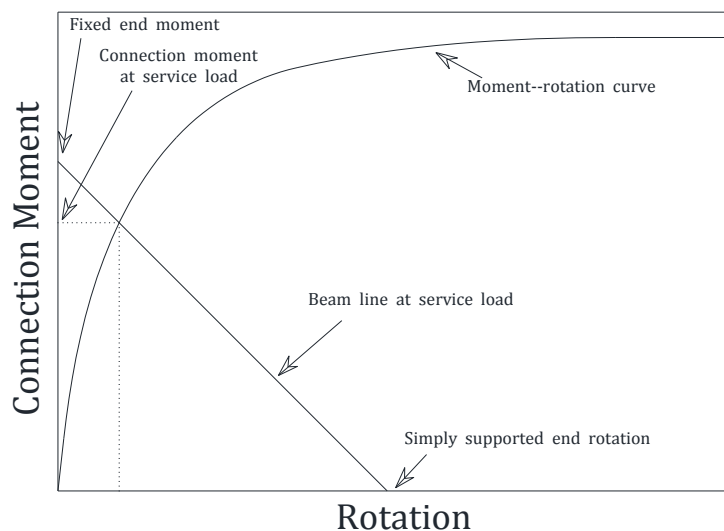


Fig. 2 Beam line theory

it includes the Ramberg Osgood Model. Therefore, the Richard Model Parameters are transformed to those of Ramberg Osgood without losing any accuracy. The slab is modeled by near-rigid struts, as considered in the FEMA report. Each node is considered to have six degrees of freedom.

The 3- and 10-level buildings with PRC will be denoted as Models PR1 and PR2, respectively, and in general, they will be referred as the PR Models. As stated earlier, several rigidities of the connections are considered; three for PRC oriented in the E-W direction and one for the N-S direction; the first connection rigidity level (which is also the only used in the N-S direction) resulted from the design of the connections for gravity loads and approximately corresponds to a relative rigidity of 0.2 ($T = 0.2$) where double web angles were used. This definition of rigidity is according to the beam line theory (Disque 1964) and the Richard Model (Richard 1993) (Fig. 2). The other rigidities correspond to T ratios of 0.4 and 0.6. Double web angle (DWA) and double web top and seat angle (DWATS) were used. Typical DWA and DWATS connections are shown in Fig. 3(a) and (b), respectively, while the details of the connection components for the three levels of rigidity of the two models are given in Table 3.

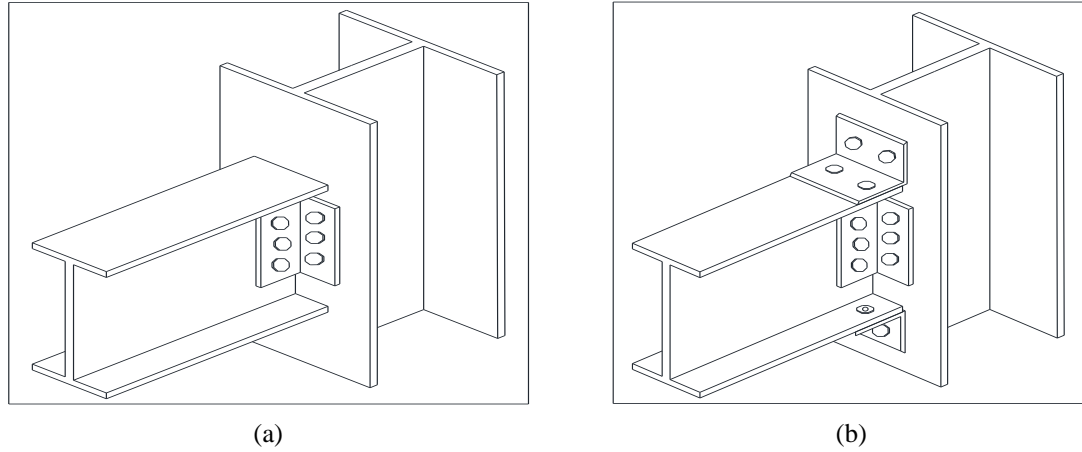


Fig. 3 PRC, (a) DWA; (b) DWATS

4.3 Seismic motions

Dynamic responses of a structure excited by different earthquake time histories, even when they are normalized in terms of the same pseudo-acceleration (S_a) or in terms of any other response parameter, are expected to be different, reflecting their different frequency content. Thus, evaluating structural responses excited by an earthquake may not reflect the behavior properly. To study the responses of the models comprehensively and to make meaningful conclusions, they are excited by twenty recorded earthquake motions in time domain with different frequency content, recorded at different locations. The characteristics of the earthquakes are given in Table 4 for the N - S direction and their elastic response spectra in Fig. 4. As shown in the table, the predominant periods of the earthquakes for the N - S direction vary from 0.11 to 0.62 s.

The predominant period for each earthquake is defined as the period where the largest peak in the pseudo-acceleration elastic response spectrum occurs. The earthquake time histories were obtained from the Data Sets of the National Strong Motion Program (NSMP) of the United States Geological Surveys (USGS). Additional information on these earthquakes can be obtained from this data base.

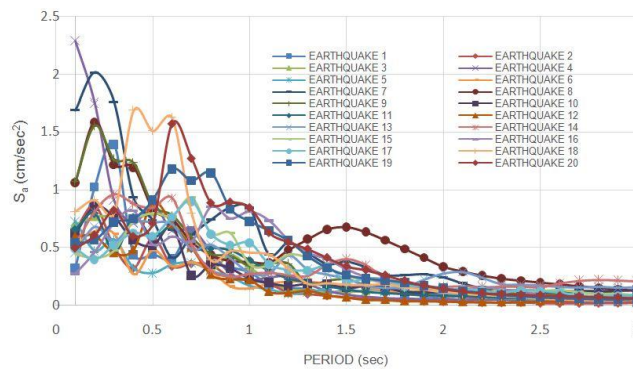
The building models behave essentially elastic under the action of any of the earthquake motions. In order to have different levels of deformation as well as moderate and inelastic behavior, the earthquakes are scaled in terms of pseudo-accelerations evaluated at the fundamental period of the structure ($S_a(T_1)$) for values of S_a ranging from 0.2 g to 1.2 g with increments of 0.2 g, according to the following equation

$$S_a = \sqrt{\frac{S_{a,EW}^2 + S_{a,NS}^2}{2}} \quad (1)$$

where, for each seismic record, $S_{a,EW}$ and $S_{a,NS}$ are the ordinate of the pseudo-aceleración spectra for the E - W and N - S components, respectively. The maximum considered value of S_a is 1.2 g since for larger values collapse mechanisms were developed for some strong motion particularly for the 10-level building.

Table 4 Earthquake records, *N-S* component

No	Place	Date	Station	<i>T</i> (sec)	ED (km)	<i>M</i>	PGA (cm/sec ²)
1	Landers, CA	28/06/1992	Fun Valley, Reservoir 361	0.11	31	7.3	213
2	MammothLakes, CA	27/05/1980	Convict Creek	0.16	11.9	6.3	316
3	Victoria	09/06/1980	Cerro Prieto	0.16	37	6.1	613
4	Parkfield, CA	28/09/2004	Parkfield; Joaquin Canyon	0.17	14.8	6.0	609
5	PugetSound, WA	29/04/1965	Olympia Hwy Test Lab	0.17	89	6.5	216
6	Long Beach, CA	10/03/1933	UtilitiesBldg, Long Beach	0.20	29	6.3	219
7	Sierra El Mayor, Mexico	04/04/2010	El centro, CA	0.21	77.3	7.2	544
8	Petrolia/Cape Mendocino, CA	25/04/1992	Centerville Beach, Naval Facility	0.21	22	7.2	471
9	Morgan Hill	24/04/1984	GilroyArraySta #4	0.22	38	6.2	395
10	Western Washington	13/04/1949	Olympia Hwy Test Lab	0.22	39	7.1	295
11	San Fernando	09/02/1971	Castaic - Old Ridge Route	0.23	24	6.6	328
12	MammothLakes, CA	25/05/1980	Long Valley Dam	0.24	12.7	6.5	418
13	El Centro	18/05/1940	El Centro - ImpVallIrrDist	0.27	12	7.0	350
14	Loma Prieta, CA	18/10/1989	Palo Alto	0.29	47	6.9	378
15	Santa Barbara, CA	13/08/1978	UCSB Goleta FF	0.36	14	5.1	361
16	Coalinga, CA	02/05/1983	ParkfieldFaultZone 14	0.39	38	6.2	269
17	Imperial Valley, CA	15/10/1979	Chihuahua	0.40	19	6.5	262
18	Northridge, CA	17/01/1994	Canoga Park, Santa Susana	0.60	15.8	6.7	602
19	Offshore Northern, CA	10/01/2010	Ferndale, CA	0.61	42.9	6.5	431
20	Joshua Tree, CA	23/04/1992	Indio, Jackson Road	0.62	25.6	6.1	400

Fig. 4 Elastic response spectra *N-S* direction

4.4 The Richard model

Connections are structural elements that transmit resultant stresses between beams and columns. For the case of PRC their rigidity is generally represented by the bending moment acting on them

and the corresponding relative rotation. Many mathematical forms to define the bending moment-relative rotation relationship (referred as $M-\theta$ curve) for PRC are available in the literature. They include the piecewise linear, the polynomial, the exponential, the B-spline, and the Richard model (Richard and Abbot 1975, Richard 1993). The Richard model is a four-parameter model which was developed using actual worldwide test data and is adopted in this study.

When a connection is defined in terms of member sizes, bolts and/or welds, a commercially available computer program, known as PRCONN, is available to generate the appropriate $M-\theta$ curve using the Richard model. This program is used in this study to develop the required $M-\theta$ curve. According to the Richard model, the $M-\theta$ curve is given by

$$M = \frac{(K - K_p) \theta}{\left(1 + \left|\frac{(K - K_p)\theta}{M_0}\right|^N\right)^{\frac{1}{N}}} + K_p \theta \quad (2)$$

where K is the initial or elastic stiffness, K_p is the plastic stiffness, M_0 is the reference moment, and N is the curve shape parameter. The loading process and the physical definition of these parameters are shown in Fig. 5. The term “increasing N ” in this figure means that the $M-\theta$ curve tends to be bi-linear as N increases. The parameters of the Richard’s Model for the SR connections used in this study are presented in Table 5.

Eq. (2) represents the $M-\theta$ curve when the load is increasing monotonically. When a structure is excited by dynamic or seismic loading, some of the connections are expected to be loading and others are expected to be unloading and reloading. Experimental and theoretical studies related to the unloading and reloading behavior of the $M-\theta$ curve are rare. This subject has been addressed in the literature (Disque 1964, Colson 1991). For the present study, the unloading and reloading behavior of the $M-\theta$ curves is essential. As in other investigations (Reyes-Salazar and Haldar 1999, 2000, 2001a, b) in this paper, the monotonic loading behavior is represented by the Richard curve and the Masing rule is used to theoretically develop the unloading and reloading sections of the $M-\theta$ curve. Using the Masing rule and the Richard Model represented by Eq. (2), the mathematical representation for the unloading and reloading behavior of a connection can be expressed as

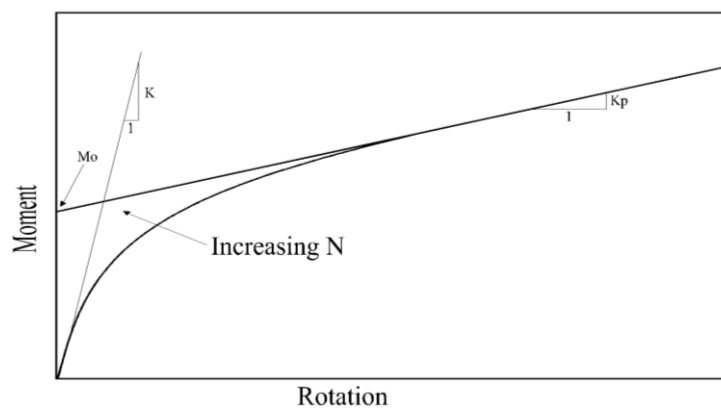


Fig. 5 Parameters of the Richard’s Model

$$M = M_a - \frac{(K - K_p)(\theta_a - \theta)}{\left(1 + \left|\frac{(K - K_p)(\theta_a - \theta)}{2M_0}\right|^N\right)^{\frac{1}{N}}} - K_p(\theta_a - \theta) \quad (3)$$

The loading, unloading and the reloading at PR are illustrated in Fig. 6. If (M_b, θ_b) is the next reversal point, as shown in the figure, the reloading relation between M and θ can be obtained by simply replacing (M_a, θ_a) with (M_b, θ_b) in Eq. (3). Thus, Eq. (2) is used if the connection is loading; if it is unloading or reloading, Eq. (3) should be used instead.

Table 5 Richard parameters for the SR connections

T ratio	Section	K (kip-in/rad)	K_p (kip-in/rad)	M_o (kip-in/rad)	N
0.2	W16×26	8.25×10^4	2.91×10^3	3.61×10^2	1.5
	W18×35	8.38×10^4	3.08×10^3	3.76×10^2	1.6
0.4	W16×26	1.79×10^5	7.67×10^3	5.72×10^2	2.1
	W18×35	2.31×10^5	9.84×10^3	6.55×10^2	2.1
0.6	W16×26	5.01×10^5	1.19×10^4	9.74×10^2	1.3
	W18×35	7.06×10^5	1.65×10^4	1.21×10^3	1.3

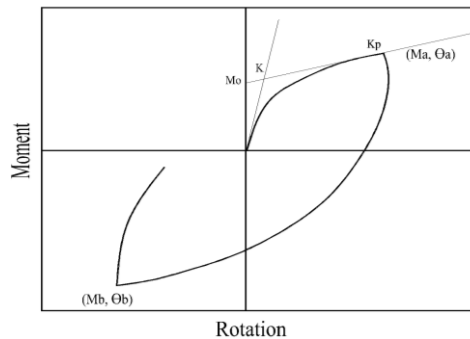


Fig. 6 Loading, unloading and reloading at PR connections

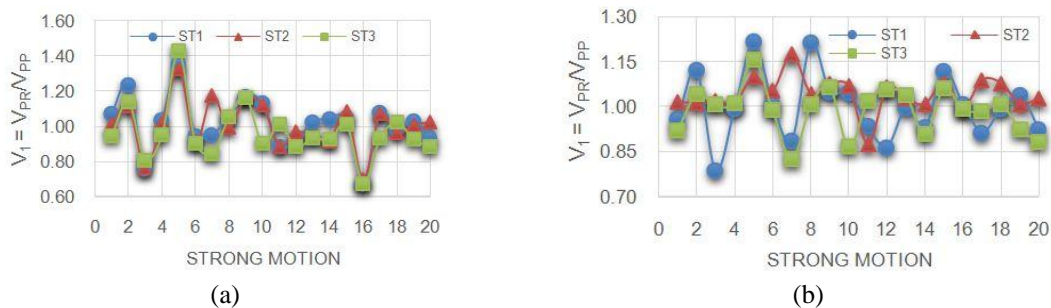


Fig. 7 V_1 ratio, E - W direction, 3-level building, $T = 0.2$; (a) $S_a = 0.2$ g; (b) $S_a = 0.4$ g; (c) $S_a = 0.6$ g; (d) $S_a = 0.8$ g; (e) $S_a = 1.0$ g; (f) $S_a = 1.2$ g

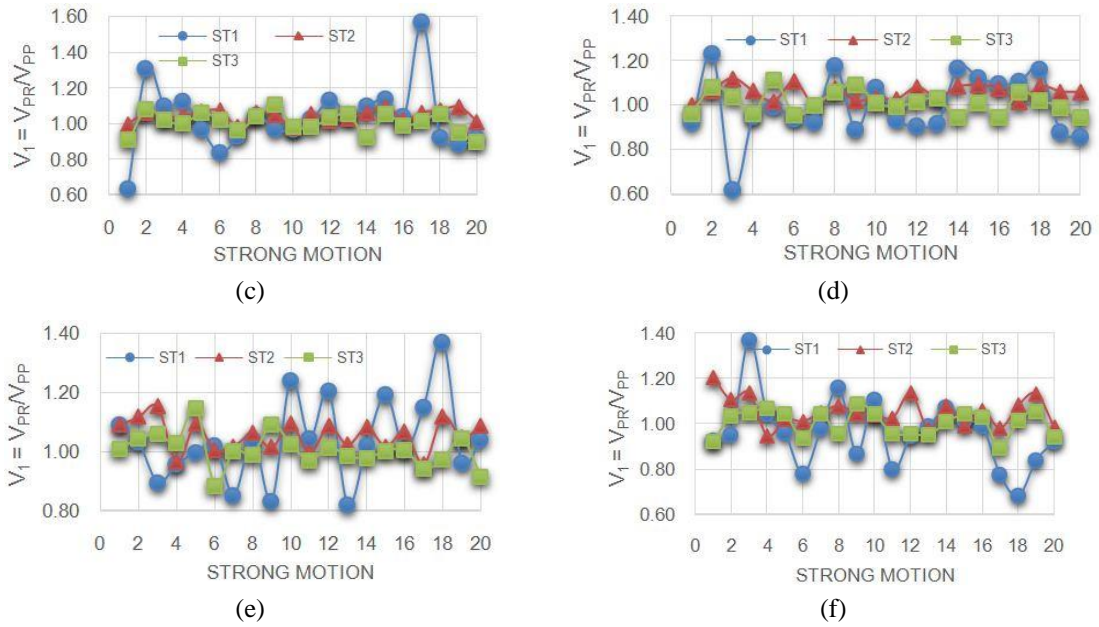


Fig. 7 Continued

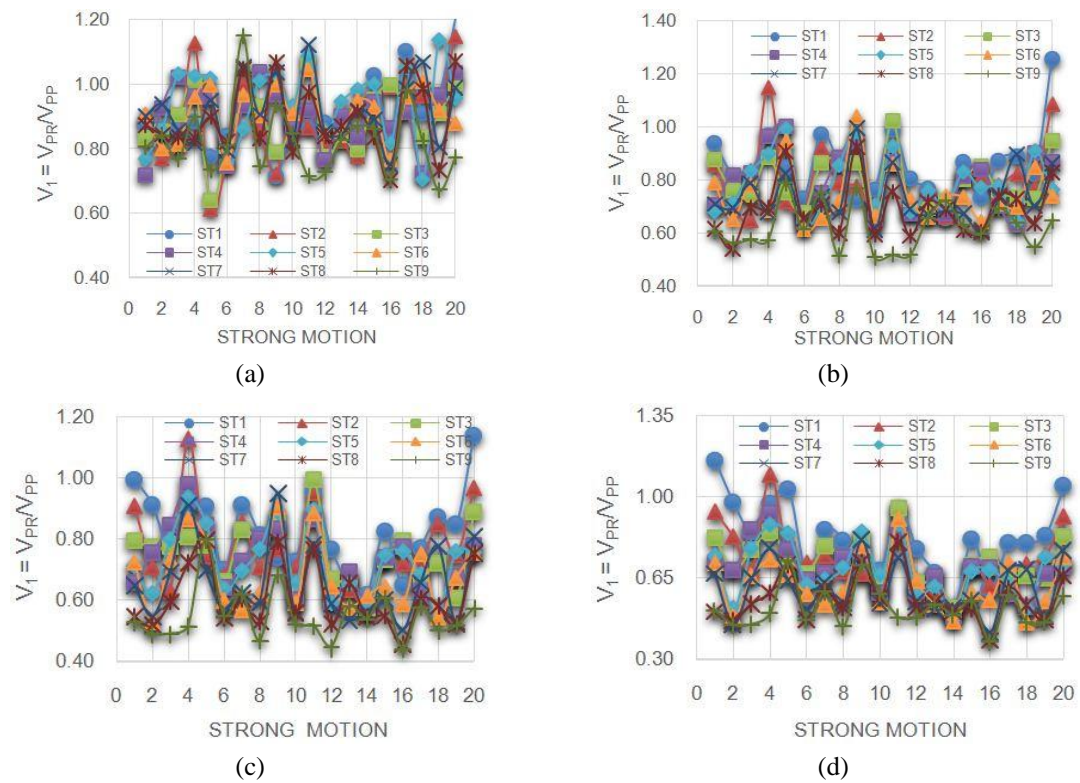


Fig. 8 V_1 ratio, E-W direction, 10-level building, $T = 0.2$; (a) $S_a = 0.2$ g; (b) $S_a = 0.4$ g; (c) $S_a = 0.6$ g; (d) $S_a = 0.8$ g; (e) $S_a = 1.0$ g; (f) $S_a = 1.2$ g

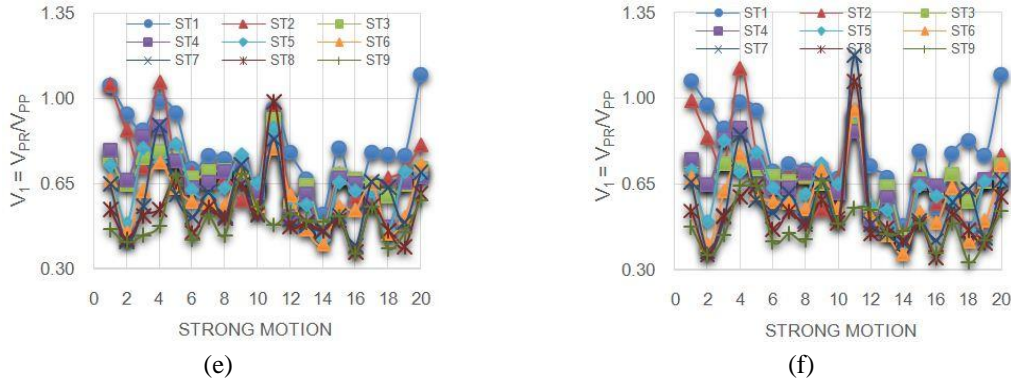


Fig. 8 Continued

5. Results in terms of global response parameters

In this section of the paper, the seismic responses in terms of global response parameters, namely, interstory shears and interstory displacements, of the steel buildings with interior PRC are estimated and compared with those of the corresponding buildings with interior PPC.

5.1 Interstory base shear

To make the comparison between interstory shears of the PRC and PPC buildings the following ratio is used

$$V_1 = \frac{V_{PR}}{V_{PP}} \quad (4)$$

where, V_{PR} and V_{PP} represent the interstory shears for the steel buildings with PRC and PPC, respectively. Thus, a value of V_1 larger than unity will indicate that the interstory shear is larger for the models with PRC. Results of V_1 , for S_a values ranging from 0.2 g through 1.2 g, $T = 0.2$ and the $E-W$ direction, are presented in Fig. 7 and Fig. 8 for the 3- and 10-level models, respectively. In these figures, the symbol “ST” stands for the story level. It can be observed that for a given building, S_a value, and interstory, the magnitude of V_1 significantly varies from one seismic motion to another, even though the model deformation was approximately the same in terms of S_a for each seismic motion. It reflects the effect of the frequency content of the seismic motions and the contribution of several vibration modes to the structural response. It is also observed that for the 3-level building, V_1 takes values smaller than unity approximately in half of the cases indicating that the interstory shears can be smaller for the buildings with PRC; values smaller than 0.7 are observed in many cases. For the 10-level building, unlike the 3-level building, V_1 is smaller than unity, practically in all cases, values smaller of up to 0.4 are observed.

Plots similar to those of Figs. 7 and 8 were also developed for the $N-S$ direction for a T ratio of 0.2 as well as for the other two values of the T ratio (0.4 and 0.6) for the $E-W$ direction but the results are not shown; only the fundamental statistics are presented. The mean value (μ) and coefficient of variation (δ) of V_1 are given in Tables 6 and 7 for the 3- and 10-level buildings, respectively. It can be observed that for the 3-level building and the $N-S$ direction, the averages of

Table 6 V_1 values, 3-level building

T	D S		S_d/g											
	I	T	0.2		0.4		0.6		0.8		1.0		1.2	
	R		μ	δ	μ	δ	μ	δ	μ	δ	μ	δ	μ	δ
0.2	N	1	1.03	14	1.03	10	1.02	7	1.02	9	1.03	8	1.02	7
	S	2	1.01	14	1.03	9	1.04	6	1.05	5	1.06	3	1.05	4
		3	1.00	15	1.01	8	1.04	6	1.01	6	0.97	6	0.98	7
		ALL	1.01	14	1.02	9	1.03	6	1.03	7	1.02	6	1.02	6
	E	1	0.97	14	0.95	10	0.99	17	0.94	14	0.99	13	0.91	15
W	2	0.96	13	0.99	6	0.99	3	1.00	3	1.01	5	1.00	6	
	3	0.92	15	0.94	8	0.96	6	0.96	5	0.96	6	0.95	6	
	ALL	0.95	14	0.96	8	0.98	9	0.97	7	0.99	8	0.95	9	
0.4	E	1	0.99	19	0.97	14	0.99	15	1.05	15	1.10	17	0.93	15
	W	2	0.98	18	1.04	6	1.04	6	1.06	4	1.06	6	1.06	8
		3	0.90	25	0.95	9	0.96	7	0.99	6	0.98	7	0.98	7
		ALL	0.96	21	0.99	10	1.00	9	1.03	8	1.05	10	0.99	10
0.6	E	1	0.94	25	0.95	16	1.02	11	1.03	20	1.08	16	0.98	15
	W	2	0.93	24	1.03	11	1.06	8	1.07	5	1.07	7	1.08	9
		3	0.84	28	0.91	11	0.94	9	0.97	8	0.97	8	0.96	9
		ALL	0.90	26	0.96	13	1.01	9	1.02	11	1.04	10	1.01	11

the mean values of V_1 are slightly larger than unity. For the 3-level building and the E - W direction, the averages of the mean values are slightly smaller than unity in most of the cases. Thus, in general, it can be said that, for the 3-level building, the interstory shears are similar for the buildings with PRC and PPC.

For the 10-level building (Table 7), unlike the case of the 3-story building, the mean values are smaller than unity practically in all cases indicating a better performance of the steel building with PRC. One of the reasons for this is that, as observed from experimental investigations, although PRC increase the lateral stiffness, they introduce a very important source of energy dissipation. Obviously, this energy dissipation doesn't exist in the buildings with PPC. Results from Table 7 also indicate that the mean values of V_1 tend to decrease as S_d or the story number increases. It is also observed for the E - W direction that the V_1 parameter tend to slightly increase as the T ratio increases. The magnitude of the averages of the mean values (which are very close and even smaller than 0.5) indicate that the reduction of the interstory shear can be considerable when PRC are used. For example, for $T = 0.2$, E - W direction and the smaller values of structural deformation, the reduction of interstory shears is 10% and 24% for $S_d/g = 0.2$ g and 0.4 g, respectively; for the intermediate level of deformation, the reductions are 30% to 34% for $S_d/g = 0.6$ g and 0.8 g, respectively; while for the largest levels of deformation the reductions are 36% to 37% for $S_d/g = 1.0$ g and 1.2 g, respectively. The results of Tables 6 and 7 also indicate that the uncertainty in the estimation of V_1 is, in general, moderate and quite similar for both buildings.

The earlier results clearly illustrate that the mean values of V_1 significantly may change from a low-rise to a middle-rise building indicating an important variation with the structural complexity.

This is explained by the fact that, for a given model, the dynamic properties, specifically their vibration mode characteristics, are quite different for the buildings with PRC and PPC; this difference may significantly vary from the 3- to the 10-level model. In addition, the fundamental period of the 10-level model (2.41 sec.) is further from the predominant periods of the strong motions than the fundamental period of the 3-level building (1.03 sec). Thus, while exciting these

Table 7 V_1 values, 10-level building

T	D I R	S T	S_a / g											
			0.2		0.4		0.6		0.8		1.0		1.2	
			μ	δ	μ	δ	μ	δ	μ	δ	μ	δ	μ	δ
0.2	N S	1	0.98	13	0.88	15	0.84	16	0.81	19	0.78	18	0.78	19
		2	0.93	12	0.80	14	0.75	18	0.72	18	0.71	19	0.69	22
		3	1.01	14	0.85	16	0.78	16	0.72	17	0.71	18	0.70	20
		4	0.96	14	0.80	15	0.72	17	0.69	19	0.66	21	0.66	21
		5	0.97	14	0.79	14	0.71	16	0.68	16	0.64	19	0.64	20
		6	0.92	14	0.75	17	0.64	16	0.61	18	0.57	21	0.56	20
		7	0.96	14	0.77	15	0.66	18	0.60	20	0.56	21	0.55	25
		8	0.89	16	0.72	18	0.62	18	0.55	20	0.53	20	0.51	24
		9	0.82	19	0.67	19	0.57	15	0.50	14	0.48	15	0.46	23
	ALL	0.94	14	0.78	16	0.70	17	0.65	18	0.63	19	0.62	22	
	E W	1	0.90	12	0.85	16	0.82	16	0.83	20	0.80	19	0.80	20
		2	0.89	15	0.80	17	0.77	18	0.74	19	0.72	22	0.71	23
		3	0.89	11	0.80	12	0.75	14	0.72	14	0.68	13	0.67	14
		4	0.90	11	0.79	15	0.73	15	0.69	16	0.67	17	0.66	18
		5	0.94	13	0.79	14	0.73	15	0.69	17	0.65	18	0.64	20
		6	0.91	9	0.75	14	0.68	17	0.62	19	0.59	18	0.58	24
		7	0.92	11	0.74	14	0.66	20	0.61	19	0.58	23	0.58	31
8		0.89	12	0.69	15	0.61	17	0.56	18	0.53	25	0.52	29	
9		0.82	13	0.62	14	0.55	15	0.52	17	0.50	17	0.48	19	
ALL	0.90	12	0.76	15	0.70	16	0.66	18	0.64	19	0.63	22		
0.4	E W	1	0.91	16	0.87	19	0.85	17	0.85	19	0.83	19	0.82	20
		2	0.91	18	0.82	18	0.78	19	0.76	20	0.74	22	0.73	23
		3	0.91	12	0.82	12	0.77	14	0.74	14	0.70	14	0.69	14
		4	0.94	12	0.82	16	0.75	16	0.70	16	0.68	17	0.68	18
		5	0.97	13	0.81	15	0.76	16	0.71	19	0.67	19	0.66	20
		6	0.94	11	0.78	16	0.70	18	0.65	20	0.61	19	0.60	24
		7	0.95	14	0.76	14	0.68	19	0.63	21	0.60	23	0.60	31
		8	0.91	14	0.71	14	0.62	16	0.58	17	0.55	23	0.54	28
		9	0.82	13	0.62	14	0.56	17	0.53	18	0.50	17	0.48	19
		ALL	0.92	14	0.78	15	0.72	17	0.68	18	0.65	19	0.64	22

Table 7 Continued

T	D I R	S T	S_a / g											
			0.2		0.4		0.6		0.8		1.0		1.2	
			μ	δ	μ	δ	μ	δ	μ	δ	μ	δ	μ	δ
0.6	E W	1	0.90	18	0.88	19	0.87	18	0.89	20	0.87	20	0.87	21
		2	0.92	19	0.84	18	0.81	18	0.78	21	0.77	22	0.76	21
		3	0.92	13	0.83	14	0.79	14	0.76	14	0.73	14	0.72	14
		4	0.95	12	0.83	16	0.77	15	0.73	16	0.70	16	0.70	17
		5	0.97	13	0.83	15	0.77	18	0.73	19	0.70	19	0.69	21
		6	0.93	12	0.79	15	0.72	18	0.67	21	0.63	19	0.62	24
		7	0.93	15	0.77	15	0.70	20	0.64	21	0.61	22	0.61	31
		8	0.88	15	0.69	14	0.62	15	0.58	16	0.57	22	0.55	27
		9	0.78	14	0.62	15	0.55	17	0.52	18	0.49	18	0.48	22
		ALL	0.91	15	0.79	16	0.73	17	0.70	18	0.67	19	0.67	22

two models (which are quite different from a dynamic point of view) by earthquakes with different frequency content (which excites the structural modes in a different way), it is expected to obtain very different values of V_1 for each model. For those cases where V_1 is smaller than unity (as in some cases of the 3-level building) or much smaller than unity (as in most of the cases of the 10-level building), a change in the mode phases of the response may have occurred allowing for larger responses for the models with PPC, particularly for the 10-level model.

5.2 Interstory displacements

The seismic responses of the buildings with PRC and PPC are now compared in terms of interstory displacements. The ratio

$$D_1 = \frac{D_{PR}}{D_{PP}} \quad (5)$$

is used to make the comparison. D_{PR} and D_{PP} represents the same as before, except that now interstory displacements are considered instead of interstory shears. D_1 values, for S_a values ranging from 0.2 g through 1.2 g, $T = 0.2$ and the *E-W* direction, are presented in Figs. 9 and 10 for the 3- and 10-level models, respectively, while the corresponding statistics for all cases are presented in Tables 8 and 9. It can be observed from the figures that the D_1 parameter is similar to V_1 in the sense that it significantly varies from one earthquake to another without showing any trend. The statistics for the 3-level building (Table 8) indicate, however, that unlike the V_1 parameter (Table 6), the D_1 mean values are smaller than unity in all cases, and obviously smaller than V_1 ; for example the minimum observed mean value of D_1 for $T = 0.4$ is 0.79 (third story, $S_a = 0.4$ and *E-W* direction) while the minimum mean value of V_1 , for the same T ratio, is 0.90 (third story, $S_a = 0.2$ and *E-W* direction). The implication of this is that the reduction of the seismic response in terms of interstory displacements is larger than that of interstory shears when PRC are considered in the buildings. From the averages of the mean values of D_1 , it can be said that the reduction on the interstory displacements for the $T = 0.2$ is about 5% in most of the cases while for

$T = 0.4$ and 0.6 it is about 10% in many cases. In addition, unlike V_1 , the D_1 mean values clearly tend to decrease as the story number increases.

For the 10-level model (Table 9), as for the case of V_1 (Table 7), the D_1 mean values may be significantly smaller than unity and tend to decrease with an increment of the story number. The results also indicate that, as for the 3-level building, the reduction of the response is, in general, larger for interstory displacements than for interstory shears when PRC are used. The uncertainty in the estimation of D_1 is moderated in most of the cases and quite similar for both models and both horizontal directions.

In summary, considering the connections of the IGF as PRC, may significantly reduce the nonlinear seismic response in terms of interstory shears or displacements. One of the reasons for this is that, as concluded from experimental investigations, PRC increase the lateral stiffness, but at the same time introduce a very important source of energy dissipation. The magnitude of the reduction significantly varies with the structural complexity of the building. Obviously, this energy dissipation doesn't exist in the buildings with interior PPC. It is expected that adding top and seat angles to increase the T ratio from 0.2 to 0.4 or 0.6, won't significantly increase that connection cost.

Even for a T ratio of 0.2, which, as stated in Section 4.2, is usually idealized as PPC, the reduction of the response in terms of interstory shear or displacements can be significant. Therefore, the dissipated energy at PRC should be considered not matter how difficult the task of estimating the seismic response becomes. Thus, PRC can be used at IGF of steel buildings with PMRF to get more economical construction, to reduce the seismic response and to make steel building more seismic load tolerant.

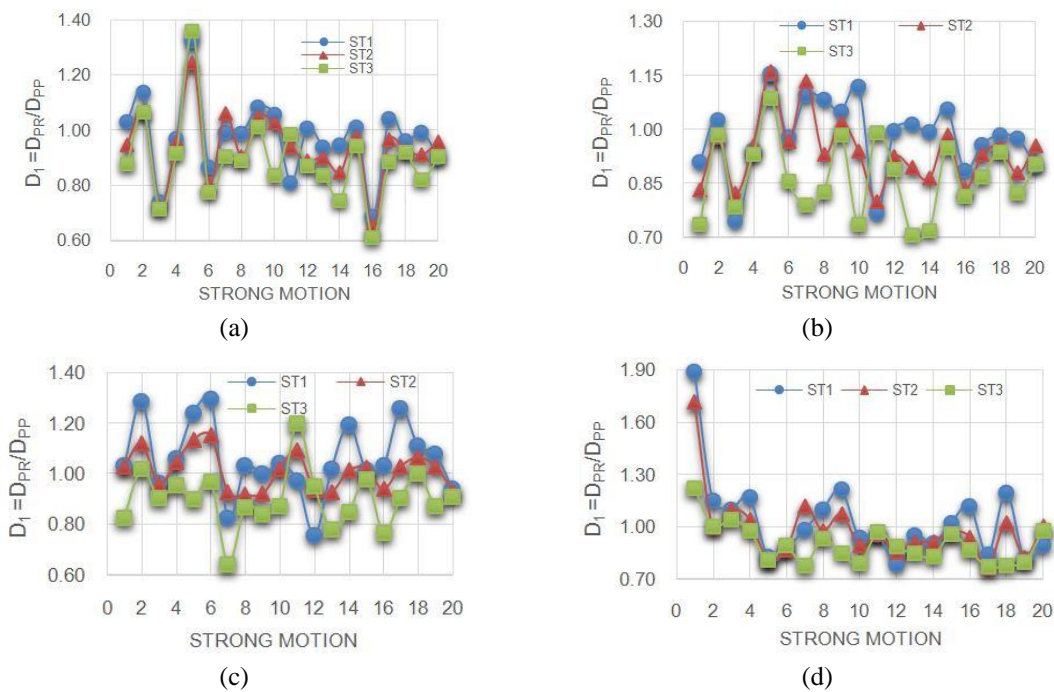


Fig. 9 D_1 ratio, E-W direction, 3-level building, $T = 0.2$; (a) $S_a = 0.2$ g; (b) $S_a = 0.4$ g; (c) $S_a = 0.6$ g; (d) $S_a = 0.8$ g; (e) $S_a = 1.0$ g; (f) $S_a = 1.2$ g

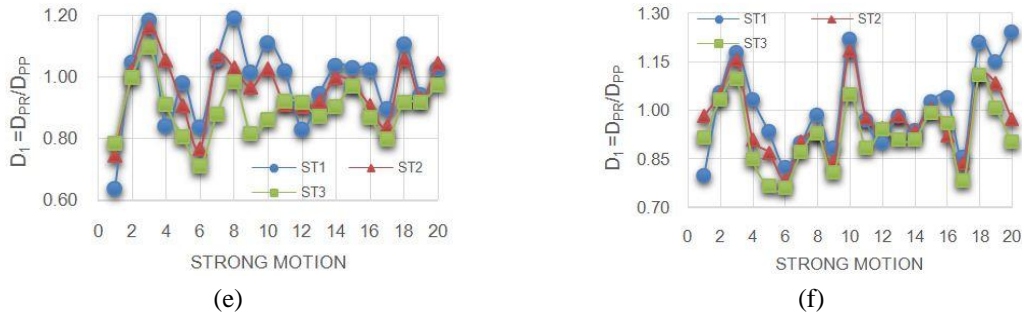


Fig. 9 Continued

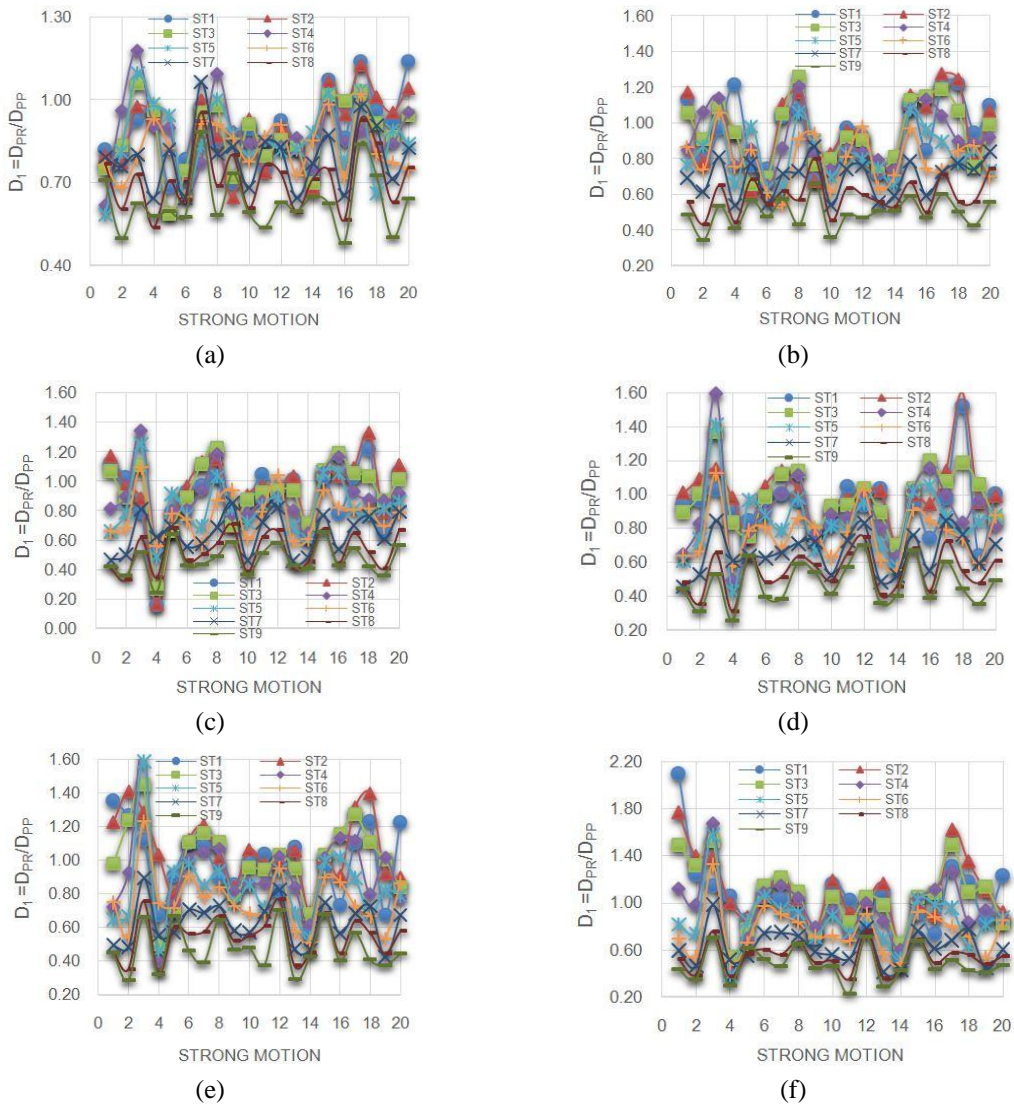


Fig. 10 D_1 ratio, E-W direction, 10-level building, $T = 0.2$; (a) $S_a = 0.2$ g; (b) $S_a = 0.4$ g; (c) $S_a = 0.6$ g; (d) $S_a = 0.8$ g; (e) $S_a = 1.0$ g; (f) $S_a = 1.2$ g

Table 8 D_I values, 3-level building

T	D I	S T	S_a/g												
			0.2		0.4		0.6		0.8		1.0		1.2		
	R		μ	δ	μ	δ	μ	δ	μ	δ	μ	δ	μ	δ	
0.2	N	1	0.98	15	1.01	18	0.98	18	0.98	18	1.05	19	1.05	20	
	S	2	0.94	14	0.97	15	0.98	16	0.95	12	0.96	17	1.00	16	
		3	0.91	15	0.94	15	0.92	14	0.88	11	0.9	16	0.92	13	
		ALL	0.94	15	0.97	16	0.96	16	0.94	14	0.97	17	0.99	16	
	E	1	0.97	14	0.98	11	1.05	15	1.01	22	1.00	12	1.02	12	
		W	2	0.94	14	0.94	10	1.01	8	0.97	19	0.97	10	0.97	9
			3	0.89	17	0.87	12	0.91	12	0.9	12	0.91	9	0.92	10
			ALL	0.93	15	0.93	11	0.99	12	0.96	18	0.96	10	0.97	10
0.4	E	1	0.97	20	0.99	13	1.07	11	1.09	28	1.04	16	1.06	18	
		2	0.90	20	0.91	11	0.99	11	0.98	21	0.95	17	0.96	15	
		3	0.83	26	0.80	17	0.83	18	0.87	15	0.86	13	0.87	15	
		ALL	0.90	22	0.90	14	0.96	13	0.98	21	0.95	15	0.96	16	
0.6	E	1	0.91	26	0.95	19	1.07	13	1.05	13	1.10	24	1.22	38	
		2	0.83	26	0.88	18	0.97	16	0.93	12	0.98	18	1.02	22	
		3	0.75	29	0.75	22	0.76	20	0.77	16	0.81	14	0.83	18	
		ALL	0.83	27	0.86	20	0.93	16	0.92	14	0.96	19	1.02	26	

6. Results in terms of local response parameters

The maximum responses of the buildings with PRC and PPC are now compared in terms of the resultant stresses at some columns of the base of the PMRF. Axial load and bending moments at exterior (EXT) and interior (INT) columns are considered (Figs. 2(c) and (f)). The parameters A_1 and M_1 given by

$$A_1 = \frac{A_{PR}}{A_{PP}} \quad (3)$$

$$M_1 = \frac{M_{PR}}{M_{PP}} \quad (4)$$

are used to make the comparison. The terms A_{PR} and A_{PP} in Eq. (3) represent the axial load on the selected columns of the buildings with PRC and PPC, respectively, while the terms M_{PR} and M_{PP} in Eq. (4) have a similar meaning, but bending moment are used instead. Plots similar to those of the V_1 and D_1 ratios were also developed for A_1 and M_1 but are not shown, only the fundamental statistics are given and discussed. The statistics for A_1 are presented in Tables 10 and 11 for the 3- and 10-level models, respectively. The results indicate that, for the 3-level model, the mean values of A_1 , are practically equal to unity, regardless the value of the T ratio, column direction (DIR), column location (LOC) and the level of deformation, implying that the axial load at the base columns of this model, on an average basis, is the same for the buildings with PRC and

PPC. For the 10-building, however, the A_1 mean values may be significantly smaller than unity, indicating that axial loads may be significantly reduced when PRC are used. Values smaller than 0.70 are observed in many cases implying an axial load reduction larger than 35%. From the average of the mean values reductions of about 10% are observed in some cases. The uncertainty in the estimation of A_1 is moderate, which is, in general, larger for the 10- than for the 3-level building.

Table 9 D_I values, 10-level building

T	D I R	S T	S_a / g											
			0.2		0.4		0.6		0.8		1.0		1.2	
			μ	δ	μ	δ	μ	δ	μ	δ	μ	δ	μ	δ
0.2	N S	1	0.93	12	0.90	17	0.91	28	0.93	21	0.95	22	0.95	25
		2	0.96	13	0.98	17	0.99	28	1.02	24	1.06	26	1.09	27
		3	0.96	13	0.97	15	0.96	30	1.03	29	1.07	29	1.08	30
		4	0.88	14	0.88	16	0.91	27	0.95	32	0.96	31	0.96	34
		5	0.84	13	0.82	15	0.81	29	0.86	30	0.87	31	0.84	36
		6	0.86	11	0.81	14	0.76	30	0.81	29	0.83	34	0.80	38
		7	0.85	14	0.75	16	0.67	28	0.66	22	0.66	28	0.67	34
		8	0.80	16	0.69	16	0.59	26	0.59	21	0.60	25	0.61	30
		9	0.76	17	0.68	15	0.59	24	0.59	18	0.61	24	0.63	29
	ALL	0.87	14	0.83	16	0.80	28	0.83	25	0.85	28	0.85	31	
	E W	1	0.89	15	0.95	19	0.89	26	0.93	20	0.98	22	1.05	31
		2	0.88	17	0.95	22	0.94	27	1.01	18	1.06	19	1.11	25
		3	0.87	15	0.95	19	0.93	24	0.99	17	1.00	22	1.05	26
		4	0.87	15	0.91	17	0.90	20	0.90	26	0.92	28	0.95	28
		5	0.86	15	0.83	17	0.83	21	0.83	25	0.84	28	0.85	28
		6	0.83	12	0.79	17	0.77	20	0.76	20	0.76	22	0.76	27
		7	0.79	14	0.70	15	0.65	21	0.66	18	0.63	20	0.62	23
		8	0.71	16	0.59	17	0.53	24	0.54	23	0.55	23	0.53	23
9		0.63	17	0.50	16	0.47	22	0.47	26	0.47	28	0.47	29	
ALL	0.81	15	0.80	18	0.77	23	0.79	21	0.80	24	0.82	27		
0.4	E W	1	0.86	19	0.95	23	0.90	28	0.96	20	0.98	25	1.03	31
		2	0.82	20	0.93	23	0.91	28	1.01	20	1.05	22	1.08	26
		3	0.83	16	0.91	19	0.89	25	0.97	18	0.98	23	1.02	26
		4	0.84	16	0.87	19	0.86	21	0.87	26	0.90	27	0.92	27
		5	0.84	17	0.80	19	0.80	23	0.80	26	0.81	28	0.83	28
		6	0.80	15	0.76	17	0.74	22	0.73	21	0.71	21	0.72	25
		7	0.74	19	0.66	17	0.61	22	0.61	18	0.58	18	0.58	22
		8	0.65	18	0.55	18	0.49	23	0.49	23	0.49	22	0.48	22
		9	0.56	19	0.45	19	0.41	22	0.41	25	0.40	25	0.41	28
		ALL	0.77	18	0.76	19	0.73	24	0.76	22	0.77	23	0.79	26

Table 9 Continued

T	D I R	S T	S_a/g											
			0.2		0.4		0.6		0.8		1.0		1.2	
			μ	δ	μ	δ	μ	δ	μ	δ	μ	δ	μ	δ
0.6	E W	1	0.84	22	0.93	22	0.89	29	0.96	21	1.01	32	1.03	33
		2	0.79	21	0.89	23	0.88	29	0.96	22	1.03	28	1.05	28
		3	0.79	17	0.87	20	0.85	25	0.92	19	0.96	26	0.98	27
		4	0.80	16	0.81	20	0.82	22	0.83	26	0.86	27	0.88	27
		5	0.79	17	0.76	19	0.76	24	0.75	26	0.76	27	0.78	27
		6	0.75	16	0.72	17	0.69	23	0.67	21	0.66	19	0.67	23
		7	0.69	23	0.61	20	0.57	22	0.56	20	0.53	17	0.54	19
		8	0.59	21	0.50	20	0.44	22	0.44	22	0.43	19	0.42	18
		9	0.49	20	0.39	19	0.35	21	0.35	24	0.34	22	0.34	24
	ALL	0.73	19	0.72	20	0.69	24	0.72	22	0.73	24	0.74	25	

The mean values of M_1 are given in Tables 12 and 13, for the 3- and 10-level buildings, respectively. For the 3-level building, it can be observed that, as for the A_1 parameter, the mean values of M_1 are very close to unity in most of the cases, however, unlike A_1 , M_1 mean values are observed to be larger than 1.10 in a few cases. For the 10-level model, unlike the case of the 3-level model, the mean values of M_1 are smaller than unity in all cases, which tend to decrease as S_a increases. Averages of the mean values are observed to be about 0.75 in some cases, implying a reduction of 25% in bending moments. The uncertainty in the estimation of M_1 is moderate and is quite similar for the 3- and 10-level buildings.

Table 10 A_1 values, 3-level building

T	D I R	L O C	S_a/g											
			0.2		0.4		0.6		0.8		1.0		1.2	
			μ	δ	μ	δ	μ	δ	μ	δ	μ	δ	μ	δ
0.2	N S	EXT	0.97	6	0.98	5	0.99	5	0.97	3	1.00	6	1.00	5
		INT	1.00	1	1.02	2	1.00	2	1.00	3	1.00	2	1.01	3
	E W	EXT	0.96	6	0.98	3	0.98	2	0.98	4	0.98	4	0.99	3
		INT	0.99	1	0.99	2	0.99	2	1.00	2	0.99	3	1.00	2
		ALL	0.98	4	0.99	3	0.99	3	0.99	3	0.99	4	1.00	3
0.4	E W	EXT	0.94	9	0.96	4	0.96	4	0.97	4	0.96	4	0.97	5
		INT	0.99	2	0.99	2	1.00	3	1.00	2	1.00	4	1.00	3
		ALL	0.97	6	0.98	3	0.98	4	0.99	3	0.98	4	0.99	4
0.6	E W	EXT	0.90	10	0.94	6	0.94	4	0.96	4	0.97	4	0.98	6
		INT	0.99	2	0.99	2	1.01	3	1.00	2	1.01	3	1.01	3
	ALL	0.95	6	0.97	4	0.98	4	0.98	3	0.99	3.5	1.00	5	

Table 11 A_T values, 10-level building

T	D L		S_a / g											
	I	O	0.2		0.4		0.6		0.8		1.0		1.2	
	R	C	μ	δ	μ	δ	μ	δ	μ	δ	μ	δ	μ	δ
0.2	N	EXT	0.95	9	0.81	12	0.74	17	0.70	25	0.68	32	0.69	37
	S	INT	1.00	4	1.01	4	1.02	7	1.03	11	1.02	13	1.01	24
	E	EXT	0.98	5	0.99	5	1.00	9	0.98	18	0.95	22	0.98	26
	W	INT	1.01	3	1.03	3	1.04	7	1.02	10	0.95	13	1.01	15
		ALL	0.98	6	0.96	6	0.95	10	0.93	16	0.90	20	0.92	26
0.4	E	EXT	1.02	6	1.00	7	1.00	11	0.98	19	0.95	22	0.98	26
	W	INT	1.02	1	1.03	2	1.04	7	1.06	9	1.03	13	1.01	15
		ALL	1.02	4	1.02	5	1.02	9	1.02	14	0.99	18	1.00	21
0.6	E	EXT	1.01	6	1.00	8	1.00	12	0.98	18	0.95	21	0.97	25
	W	INT	1.02	1	1.03	2	1.05	7	1.06	9	1.03	13	1.00	14
		ALL	1.02	4	1.02	5	1.03	10	1.02	14	0.99	17	0.99	20

Table 12 M_1 values, 3-level building

T	D L		S_a / g											
	I	O	0.2		0.4		0.6		0.8		1.0		1.2	
	R	C	μ	δ	μ	δ	μ	δ	μ	δ	μ	δ	μ	Δ
0.2	N	EXT	0.99	14	1.00	11	0.99	27	1.07	20	0.98	14	1.05	19
	S	INT	0.99	15	0.95	26	1.04	21	1.07	24	0.99	14	1.03	20
	E	EXT	0.98	16	1.01	17	1.10	21	1.06	23	1.14	17	1.06	18
	W	INT	0.98	15	1.02	20	0.98	15	1.13	14	1.08	29	1.13	22
		ALL	0.99	15	1.00	19	1.03	21	1.08	20	1.05	19	1.07	20
0.4	E	EXT	0.98	19	1.04	20	1.10	16	1.10	21	1.23	26	1.16	26
	W	INT	0.98	19	1.03	25	1.04	25	1.13	18	1.13	32	1.14	26
		ALL	0.98	19	1.04	23	1.07	21	1.12	20	1.18	29	1.15	26
0.6	E	EXT	0.93	26	0.97	17	1.09	24	1.10	23	1.20	20	1.09	17
	W	INT	0.93	26	1.02	27	1.00	28	1.11	19	1.12	28	1.22	25
		ALL	0.93	26	1.00	22	1.05	26	1.11	21	1.16	24	1.16	21

From a comparison of the values of V_1 and D_1 with those of A_1 and M_1 , it is observed that the reduction in the response is larger for global than for local response parameters, which in turn depends on the particular local response parameter being considered and the structural element location. The differences between the level of global and local reductions or between axial load and bending moments are produced by many factors. For the case of symmetric buildings, interstory shear (global parameter), or bending moments at base columns (local parameter), are non-collinear. Thus, for a given direction these parameters won't be affected by the horizontal component perpendicular to the direction under consideration. However, collinear local response

Table 13 M_1 values, 10-level building

T	D L		S_a / g											
	I O		0.2		0.4		0.6		0.8		1.0		1.2	
	R C		μ	δ	μ	δ	μ	δ	μ	δ	μ	δ	μ	Δ
0.2	N	EXT	0.91	11	0.84	16	0.85	23	0.83	26	0.75	22	0.79	26
	S	INT	0.90	12	0.83	16	0.81	18	0.80	16	0.77	18	0.73	22
	E	EXT	0.84	14	0.82	19	0.82	18	0.78	16	0.75	26	0.72	21
	W	INT	0.85	14	0.83	17	0.80	19	0.75	20	0.79	28	0.74	27
		ALL	0.88	13	0.83	17	0.82	20	0.79	20	0.77	24	0.75	24
0.4	E	EXT	0.83	18	0.80	20	0.83	21	0.79	16	0.77	28	0.75	26
	W	INT	0.83	18	0.81	20	0.80	22	0.80	24	0.83	31	0.77	24
		ALL	0.83	18	0.81	20	0.82	22	0.80	20	0.80	30	0.76	25
0.6	E	EXT	0.80	21	0.83	26	0.83	24	0.82	20	0.80	35	0.74	24
	W	INT	0.82	22	0.84	28	0.80	21	0.80	28	0.83	33	0.79	24
		ALL	0.81	22	0.84	27	0.82	23	0.81	24	0.82	34	0.77	24

parameters, like axial load on columns, are affected by the action of the three components. The contribution of each component to the axial load on an specific column may be in phase each other during some periods of time, but may be out of phase for some others periods.

These *in phase* or *out in phase* contributions may be quite different for the PR and PP models. This situation does not occur for non-collinear parameters. Moreover, the axial load in a given column produced by seismic lateral load is also affected by the distance from their location to the center of stiffness of the structure.

7. Conclusions

The nonlinear seismic responses of steel buildings with perimeter moment resisting frames (PMRF) and interior gravity frames (IGF) are estimated, first considering the interior connections as partially restrained (PRC) and then as perfectly pinned (PPC); after that the ratio of these two responses is calculated. The 3- and 10-level steel buildings used in the SAC steel project and several strong motion records are considered. The ratio is estimated in terms of global response parameters (interstory shear and displacements) and in terms of local response parameters (axial loads and bending moments at some base columns). The relative stiffness of PRC is represented by the T ratio, which is calculated according to the Beam Line Theory.

The results of the numerical study indicate that the seismic responses can be significantly reduced when interior connections are considered as PRC, confirming what observed from experimental investigations: PRC slightly increase the lateral stiffness, but at the same time they introduce a very important source of energy dissipation. The level of the reduction, in general, significantly varies from one earthquake to another, from one model to another, from one story to another as well as with the level of structural deformation, the type of response parameter under consideration, and the location of the structural elements. The reduction of the response is larger for global than for local response parameters; for example, the maximum observed averages of the

mean values for interstory shear and displacements can be smaller than 0.7, implying a reduction larger than 30%, while the corresponding maximum reductions for axial load and bending moments at base columns are about 10% and 20%, respectively. The magnitude of the reduction is much larger for medium- than for low-rise buildings, which indicates that the structural complexity has a considerable effect on the nonlinear responses of steel buildings with PRC and PPC.

It can be concluded that, the dissipated energy at interior PRC has an important effect on the reduction of the seismic response and should not be neglected. It is expected that adding top and seat angles to increase the T ratio from 0.2 to 0.4 or 0.6, won't significantly increase that connection cost. Even for a T ratio of 0.2, which is usually idealized as PPC, the reduction of the response can be significant. Therefore, the dissipated energy at PRC should be considered not matter how difficult the task of estimating the seismic response becomes. Thus, PRC can be used at IGF of steel buildings with PMRF to get more economical construction, to reduce the seismic response and to make steel building more seismic load tolerant. Much more research is needed to consider other aspects of the problem to reach more general conclusions.

Acknowledgments

This paper is based on work supported by La Universidad Autónoma de Sinaloa (UAS) under grant PROFAPI-2014/174. Any opinions, findings, conclusions, or recommendations expressed in this publication are those of the authors and do not necessarily reflect the views of the sponsors.

References

- Bjorhovde, R., Colson, A. and Brozzetti, J. (1990), "Classification system for beam-to-column connections", *J. Struct. Eng. ASCE*, **116**(11), 3059-3076.
- Black, E.F. (2012), "Inelastic parameter estimates for regular steel moment-resisting frame", *Eng. Struct.*, **34**, 33-39.
- BOCA (1993), (12th Edition), Building Officials & Code Administration International Inc, National Building Code.
- Bojorquez, E., Reyes-Salazar, A., Terán-Gilmore, A. and Ruiz, S.E. (2010), "Energy-based damage index for steel structures", *Steel Compos. Struct., Int. J.*, **4**(10), 331-348.
- Carr, A. (2011) "RUAUMOKO, Inelastic dynamic analysis program", Ph.D. Dissertation; University of Cantenbury, Cantenbury, England.
- Chang, H.Y., Jay Lin, C.C., Lin, K.C. and Chen, J.Y. (2009), "Role of accidental torsion in seismic reliability assessment for steel buildings", *Steel Compos. Struct., Int. J.*, **9**(5), 457-471.
- Colson, A. (1991), "Theoretical modeling of semi-rigid connections behavior", *J. Construct. Steel Res.*, **19**(3), 213-224.
- Disque, R.O. (1964), "Wind connections with simple framing", *Eng. J., AISC 1964*, **1**(3), 101-103.
- Elnashai, A.S. and Elgazhouli, A.Y. (1994), "Seismic behavior of semi-rigid steel frames", *J. Construct. Steel Res.*, **29**(1-3), 149-174.
- Elnashai, A.S., Elgazhouli, A.Y. and Denesh Ashtiani, F.A. (1998), "Response of semi-rigid steel frames to cyclic and earthquake loads", *J. Struct. Eng. ASCE*, **194**(8), 857-867.
- El-Salti, M.K. (1992), "Design of frames with partially restrained connections", Ph.D. Dissertation; University of Arizona, Tucson, AZ, USA.
- FEMA (2000), State of the Art Report on Systems Performance of Steel Moment Frames Subjected to Earthquake Ground Shaking; SAC Steel Project, Report FEMA 355C, Federal Emergency Management

Agency.

- Garcia, R., Sullivan, T.J. and Della Corte, G. (2010), "Development of a displacement-based design method for steel frame-RC wall building", *J. Earthq. Eng.*, **14**(2), 252-277.
- Gholipour, F.M., Mojtahedi, A. and Nourani, V. (2015), "Effect of semi-rigid connections in improvement of seismic performance of steel moment-resisting frames", *Steel Compos. Struct., Int. J.*, **19**(2), 467-484.
- Kishi, N., Chen, W.F., Goto, Y. and Hasan, R. (1996), "Behavior of tall buildings with mixed use of rigid and semi-rigid connections", *Comput. Struct.*, **61**(6), 1193-1206.
- Kishi, N., Chen, W.F., Goto, Y. and Matsuoka, K.G. (2003), "Design aid of semi-rigid connections for frame analysis", *Eng. J., AISC*, **30**(3), 90-107.
- Krishnan, S., Ji, C., Komatitsch, D. and Tromp, J. (2006), "Performance of two 18-storey steel moment-frame building in Southern California during two large simulated San Andres Earthquakes", *Earthq. Spectra*, **22**(4), 1035-1061.
- Leon, R.T. and Shin, K.J. (1995), "Performance of semi-rigid frames", *Am. Beyond*, 1020-1035.
- Lee, K. and Foutch, D.A. (2006), "Seismic evaluation of steel moment frames buildings designed using different R-values", *J. Struct. Eng. Div., ASCE*, **132**(9), 1461-1472.
- Liao, K.W., Wen, Y.K. and Foutch, D.A. (2007), "Evaluation of 3D steel moment frames under earthquake excitations. I: modeling", *J. Struct. Eng., ASCE*, **133**(3), 462-470.
- Liu, J. and Astaneh-Asl, A. (2000), "Cyclic tests on simple connections including effects of the slab", Report SAC/BD-00/03; SAC Joint Venture.
- López-Barraza, A., Ruiz, S.E., Reyes-Salazar, A. and Bojórquez, E. (2016), "Demands and distribution of hysteretic energy in moment resistant self-centering steel frames", *Steel Compos. Struct., Int. J.*, **20**(5), 1155-1171.
- Nader, M.N. and Astaneh-Asl, A. (1991), "Dynamic behavior of flexible, semi-rigid and rigid frames", *J. Construct. Steel Res.*, **18**(3), 179-192.
- Nguyen, P.C. and Kim, S.E. (2013), "Nonlinear elastic dynamic analysis of space steel frames with semi-rigid connections", *J. Construct. Steel Res.*, **84**, 72-81.
- Nguyen, P.C. and Kim, S.E. (2014), "Nonlinear inelastic time-history analysis of three-dimensional semi-rigid steel frames", *J. Construct. Steel Res.*, **101**, 192-206.
- Nguyen, P.C. and Kim, S.E. (2015), "Second-order spread-of-plasticity approach for nonlinear time-history analysis of space semi-rigid steel frames", *Finite Elem. Anal. Des.*, **105**, 1-15.
- Reyes-Salazar A. (2002), "Ductility and ductility reduction factors", *Struct. Eng. Mech., Int. J.*, **13**(4), 369-385.
- Reyes-Salazar, A. and Haldar, A. (1999), "Nonlinear seismic response of steel structures with semi-rigid and composite connections", *J. Construct. Steel Res.*, **51**(1), 37-59.
- Reyes-Salazar, A. and Haldar, A. (2000), "Dissipation of energy in steel frames with PR connections", *Struct. Eng. Mech., Int. J.*, **9**(3), 241-256.
- Reyes-Salazar, A. and Haldar, A. (2001a), "Energy dissipation at PR frames under seismic loading", *J. Struct. Eng. ASCE*, **127**(5), 588-593.
- Reyes-Salazar, A. and Haldar, A. (2001b), "Seismic response and energy dissipation in partially restrained and fully restrained steel frames: An analytical study", *Steel Compos. Struct., Int. J.*, **1**(4), 459-480.
- Reyes-Salazar, A., Bojórquez, E., Velazquez-Dimas, J.I., López-Barraza, A. and Rivera-Salas, J.L. (2015), "Ductility and ductility reduction factors for steel buildings considering different structural representations", *Bull. Earthq. Eng.*, **13**(6), 1749-1771.
- Rafiee, A., Talatahari, S. and Hadidi, A. (2013), "Optimum design of steel frames with semi-rigid connections using big bang-Big crunch method", *Steel Compos. Struct., Int. J.*, **14**(5), 431-451.
- Richard, R.M. and Abbott, B.J. (1975), "Versatile elastic plastic stress-strain formula", *ASCE J. Eng. Mech.*, **101**(4), 511-515.
- Richard R.M., PRCONN (1993), "Moment-rotation curves for partially restrained connections", RMR Design Group, Tucson, AZ, USA.
- Ricles, J.M., Sause, R., Garlock, M. and Zhao, C. (2001), "Post-tensioned seismic-resistant connections for steel frames", *J. Struct. Eng. ASCE*, **127**(2), 113-121.

- Sagiroglu, M. and Aydin, A.C. (2015), "Design and analysis of non-linear space frames with Semi-rigid connections", *Steel Compos. Struct., Int. J.*, **18**(6), 1405-1421.
- Shen, J. and Astaneh-Asl, A. (1999), "Hysteretic behavior of bolted angle connections", *J. Construct. Steel Res.*, **51**(3), 201-218.
- Shen, J. and Astaneh-Asl, A. (2000), "Hysteretic model of bolted-angle connections", *J. Construct. Steel Res.*, **54**(3), 317-343.
- UBC (1997), Structural Engineering Design Provisions; International Conference of Building Officials.
- Valipour, H.R. and Bradford, M.A. (2013), "Nonlinear $P-\Delta$ analysis of steel frames with semi-rigid connections", *Steel Compos. Struct., Int. J.*, **14**(1), 1-20.
- Yang, J.G. and Jeon, S.S. (2009), "Analytical model for the initial stiffness and plastic moment capacity of an unstiffened top and seat connection under a shear load", *Int. J. Steel Struct.*, **9**(3), 195-205.

CC